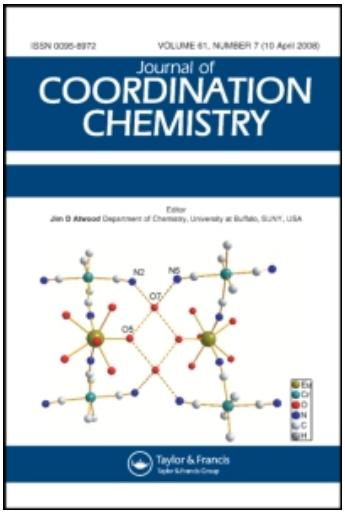

Journal of Coordination Chemistry

Publication details, including instructions for authors and subscription information:
http://www.informaworld.com/smpp/title~content=t713455674

Binuclear copper and zinc complexes possessing bio-potential ligands: synthesis, characterization, antimicrobial, SOD mimetic, DNA binding, and cleavage studies

N. Raman[a]; A. Sakthivel[a]; R. Jeyamurugan[a]
[a] Research Department of Chemistry, VHNSN College, Madurai Kamaraj University, Virudhunagar 626001, Tamil Nadu, India

Online publication date: 07 April 2010

To cite this Article Raman, N. , Sakthivel, A. and Jeyamurugan, R.(2010) 'Binuclear copper and zinc complexes possessing bio-potential ligands: synthesis, characterization, antimicrobial, SOD mimetic, DNA binding, and cleavage studies', Journal of Coordination Chemistry, 63: 6, 1080 — 1096
To link to this Article: DOI: 10.1080/00958971003699745
URL: http://dx.doi.org/10.1080/00958971003699745

Journal of Coordination Chemistry
Vol. 63, No. 6, 20 March 2010, 1080–1096

Binuclear copper and zinc complexes possessing bio-potential ligands: synthesis, characterization, antimicrobial, SOD mimetic, DNA binding, and cleavage studies

N. RAMAN*, A. SAKTHIVEL and R. JEYAMURUGAN

Research Department of Chemistry, VHNSN College, Madurai Kamaraj University, Virudhunagar 626001, Tamil Nadu, India

(*Received 20 August 2009; in final form 29 October 2009*)

Schiff bases (L) *viz*, N,N′,N″,N‴-tetra-3,4-dimethoxybenzalidene-3,3′-diaminobenzidine (TDBD), N,N′,N″,N‴-tetra-4-hydroxy-3-methoxybenzalidene-3,3′-diaminobenzidine (THMBD), and N,N′,N″,N‴-tetra-3-hydroxy-4-nitrobenzalidene-3,3′-diaminobenzidine (THNBD) afford binuclear $[M_2LCl_4]$ complexes where M = Cu(II) or Zn(II). These Schiff bases and their binuclear complexes have been characterized by analytical and spectral data showing square-planar geometry on metalation with Cu^{2+}. Intercalative binding of these complexes with DNA has been investigated by electronic absorption spectroscopy, viscosity measurements, cyclic voltammetry, and differential pulse voltammetry. Control DNA cleavage experiments using pUC19 supercoiled (SC) DNA and minor groove binder distamycin suggest that these synthesized complexes bind to the major groove. In the presence of a reducing agent like 3-mercaptopropionic acid (MPA), they show chemical nuclease activity. They also show an efficient photo-induced DNA cleavage on irradiation with a monochromatic UV light of 360 nm in the presence of inhibitors. Control experiments indicate the inhibition of cleavage in the presence of singlet oxygen quencher like sodium azide and the enhancement of cleavage in D_2O show the formation of singlet oxygen as reactive species. The superoxide dismutase (SOD)-mimetic activity of the synthesized complexes has been assessed for their ability to inhibit the reduction of nitroblue tetrazolium chloride (NBT). The complexes have promising SOD-mimetic activity. The antimicrobial results indicate that the complexes inhibit the growth of bacteria and fungi more than free ligands.

Keywords: Schiff base; Photo-cleavage; Binding constant; Antimicrobial; SOD

1. Introduction

The chemistry of multinuclear coordination metal complexes, especially of coupled system, is of special interest in various fields of science due to the interaction between metal centers lying at the crossover point of widely separated areas, physics of the magnetic materials, and polynuclear reaction sites in biological processes [1].

Artificial nucleases have potential application in the fields of molecular biological technology and drug development [2]. Transition metal complexes as synthetic metallonuclease have been studied extensively due to their diversity in the structure

*Corresponding author. Email: drn_raman@yahoo.co.in

Journal of Coordination Chemistry
ISSN 0095-8972 print/ISSN 1029-0389 online
DOI: 10.1080/00958971003699745

and reactivity [3], and some also exhibit antitumor or anti-HIV activities [4]. Binuclear or polynuclear complexes have attracted attention as artificial nuclease [5, 6] since they may demonstrate synergistic effects in the activation and recognition of active phosphodiesters and nucleic acid [7]. In nature, there are many phosphoesterases that are activated by two or more metal ions, such as 3′,5′-exonuclease from the Klenow fragment of DNA polymerase I, Rnase H from HIV reverse tranciptase C, alkaline phosphatase, P1 nuclease, and pherpholitase C. Tetrahymena ribozyme is also thought to be activated by at least two metal ions. Binuclear Co(III) and Ln(III) complexes play an important role because of their good nuclease activity [8, 9].

Binuclear Zn(II) complexes exhibit an excellent ability to cleave the phosphate ester bond of active phosphodiesters and RNA model compounds. Breslow [10] first prepared a binuclear Zn(II) complex and demonstrated that its cleaving activity toward active phosphodiester BNP (bis-*p*-nitrophenol phosphate), RNA model HPNP (2-hydroxypropyl-*p*-nitrophenyl phosphate), and UPV dinucleoside is five times more than that of the corresponding mononuclear zinc(II) complex. Deal and Burstyn [11] studied a series of macrocyclic copper(II) complexes and they have proposed bis(*p*-nitrophenyl) phosphate and DNA hydrolysis. These works tempted us to synthesize binuclear complexes and study their biological effects, such as superoxide dismutase (SOD)-mimetic activity, DNA binding, chemical nuclease, photo-induced DNA cleavage, and antimicrobial processes. We have reported a variety of mononuclear complexes [12–14], but, in this article, we prepared the bimolecular copper complexes for the first time and studied their DNA binding, redox-mediated DNA cleavage, photo-induced DNA cleavage, SOD activity, and antimicrobial activities to evaluate their biological efficiency with that of mononuclear complexes.

2. Experimental

2.1. *Chemicals*

All reagents – 3,3′-diaminobenzidene, 3,4-dimethoxybenzaldehyde, 4-hydroxy-3-methoxybenzaldehyde, 3-hydroxy-4-nitrobenzaldehyde, and copper/zinc chlorides – were from Merck and used as supplied. Anhydrous grade ethanol, DMF, and DMSO were purified according to standard procedures. Solutions of plasmid pUC19 DNA in 5 mmol NaCl/50 mmol Tris-HCl (pH 7.2) gave a ratio of UV absorbance at 260 and 280 nm, A_{260}/A_{280} of *ca* 1.8–1.9, indicating that the DNA was sufficiently free of protein contamination [15]. The concentration of DNA was measured from the band intensity at 260 nm with a known molar absorption coefficient (6600 $mol^{-1}\,cm^{-1}$) [16]. Stock solutions were kept at 4°C and used after not more than 4 days. Doubly distilled H_2O was used to prepare the buffer. The antimicrobial activities of the ligands and their complexes were carried out by the well-diffusion method.

2.2. *Physical measurements*

^{1}H-NMR spectra (300 MHz) of the samples were recorded in DMSO-d_6 by employing TMS as internal standard on a Bruker Avance DRX 300 FT-NMR spectrometer. The fast atom bombardment mass spectra of the complexes were recorded on a JEOL

SX 102/DA-6000 mass spectrometer/data system using argon/xenon (6 kV, 10 mA) as the FAB gas. The accelerating voltage was 10 kV and the spectra were recorded at room temperature using *m*-nitrobenzylalcohol (NBA) as the matrix. The IR spectra were recorded on a Shimadzu spectrophotometer from 4000 to 400 cm^{-1} using KBr pellets. The UV-Vis spectra were recorded on a Shimadzu UV-1601 spectrophotometer in DMF. Magnetic susceptibility measurements of the complexes were carried out by Gouy balance using copper sulfate as the calibrant. The purities of ligands and complexes were evaluated by thin-layer chromatography. Molar conductance of the complexes was measured using a Systronic conductivity bridge.

Electronic spectra of the complexes were recorded before and after the addition of DNA in the presence of 5 mmol Tris-HCl/50 mmol NaCl buffer (pH 7.2). The intrinsic binding constant for the interaction of complex with DNA was obtained from absorption data. A fixed concentration of the complex (10 μmol) was titrated with increasing amounts of DNA from 20 to 150 μmol. The equilibrium binding constants (K_b) for the interaction of the complexes with DNA were obtained from the absorption spectral titration data using the following equation:

$$[DNA]/(\varepsilon_a - \varepsilon_f) = [DNA/(\varepsilon_b - \varepsilon_f)] + 1/K_b(\varepsilon_b - \varepsilon_f), \quad (1)$$

where ε_a is the extinction coefficient observed for the charge transfer absorption at a given DNA concentration, ϵ_f the extinction coefficient of the complex free in solution, ε_b the extinction coefficient of the complex when fully bound to DNA, K_b the equilibrium binding constant, and [DNA] the concentration of nucleotides. A plot of $[DNA]/(\varepsilon_a - \varepsilon_f)$ *versus* [DNA] gives K_b as the ratio of the slope to the intercept.

Electrochemical studies were carried out using a CH Electrochemical analyzer, Model CHI620C, controlled by Chi620c software. CV measurements were performed using a glassy carbon working electrode, platinum wire auxiliary electrode, and Ag/AgCl reference electrode. The supporting electrolyte was 50 mmol NaCl/10 mmol Tris-HCl buffer (pH 7.2). Solutions were deoxygenated by purging with N_2 prior to measurements.

Viscometric experiments were carried out using an Oswald-type viscometer of 2 mL capacity thermostated in a water bath at $27 \pm 1^{\circ}C$. The flow rates of the buffer (10 mmol), DNA (150 μmol), and DNA in the presence of all complexes at various concentrations (5–40 μmol) were measured with a manually operated timer at least three times to agree within 0.2 s. The relative specific viscosity was calculated according to the relation $\eta = (t - t_0)/t_0$, where t_0 is the flow time for the buffer and t is the observed flow time for DNA in the presence and absence of the complexes. A plot of $(\eta/\eta^0)^{1/3}$ *versus* $1/R$, $R = ([DNA]/[complex])$, was constructed from viscosity measurements [17].

2.3. *Synthesis of ligands (L)*

N,N′,N″,N‴-tetra-3,4-dimethoxybenzalidene-3,3′-diaminobenzidine (TDBD) was synthesized by refluxing an ethanolic solution of 3,3′-diaminobenzidine (0.01 mol, 2.14 g) and 3,4-dimethoxybenzaldehyde (0.04 mol, 6.64 g) for 2 h. Upon cooling, the yellow microcrystalline compound obtained was filtered and washed with ethanol followed by diethyl ether and recrystallized from DMF and dried *in vacuo*. Yield: 65%. IR (KBr): 2840 ((methyl)–CH), 1624 (–CH=N) cm^{-1}. ^{1}H-NMR (DMSO-d_6): (phenyl multiplet) 6.4–7.2 δ(m), $\delta(OCH_3)$ 3.9(s), (–CH=N) 8.1(s): (807): *m*/*z*: 807; Anal. Calcd for

$[C_{48}H_{46}N_4O_8]$: C 71.4, H 5.7, N, 6.9; Found: C 70.8, H 5.7, N. 6.8 (%); λ_{max} in DMF, 255 and 383 nm (scheme 1).

N,N′,N″,N‴-tetra-4-hydroxy-3-methoxybenzalidene-3,3′-diaminobenzidine (THMBD) and N,N′,N″,N‴-tetra-3-hydroxy-4-nitrobenzalidene-3,3′-diaminobenzidine (THNBD) were synthesized according to the above-described procedure by the replacement of 3,4-dimethoxybenzaldehyde by 4-hydroxy-3-methoxybenzaldehyde (6.08 g) and 3-hydroxy-4-nitrobenzaldehyde (6.68 g), respectively. THMBD: Yield: 48%. IR (KBr): 3250–3500 (–OH), 2865 ((methyl)–CH), 1632 (–CH=N) cm^{-1}. ^{1}H-NMR (DMSO-d_6): (phenyl multiplet) 6.5–7.2 δ(m), (OCH_3) 3.8 δ(s), (–CH=N) 7.9 δ(s) and (–OH) 11.9 δ(s): *m/z*: 751: Anal. Calcd for $[C_{44}H_{38}N_4O_8]$ (%): C 70.3, H 5.1, N, 7.4. Found (%): C 69.8, H 5.0, N. 7.3; λ_{max} in DMF, 265 and 390 nm. THNBD: Yield: 62%. IR (KBr): 3225–3500 (–OH), 1338 (aromatic-NO_2), 1628 (–CH=N) cm^{-1}. ^{1}H-NMR (DMSO-d_6): (phenyl multiplet) 6.5–7.2 δ(m), (–CH=N) 8.5(s) and (–OH) 12.5(s); *m/z*: 811; Anal. Calcd for $[C_{40}H_{26}N_8O_{12}]$ (%): C 59.2, H 3.2, N, 13.8; Found (%): C 59.1, H 3.1, N. 12.9; λ_{max} in DMF, 256 and 395 nm.

2.4. *Synthesis of [Cu_2(TDBD)Cl_4]*

To a solution of TDBD (0.005 mol 4.03 g) in DMF, a solution of copper chloride (0.01 mol, 1.72 g) in ethanol was added, the mixture refluxed for 2 h, concentrated to one-third volume and kept at 0°C for 10 h. The solid product formed was filtered, washed several times with small amounts of ethanol and diethyl ether, and dried *in vacuo*. Yield: 74%. IR (KBr): 2839 ((methyl)-CH), 1602 (–CH=N) cm^{-1}. *m/z*: 1076, Anal. Calcd for $[Cu_2C_{48}H_{46}N_4O_8Cl_4]$ (%): Cu 11.8, C 53.5, H 4.3, N 5.2; Found (%):

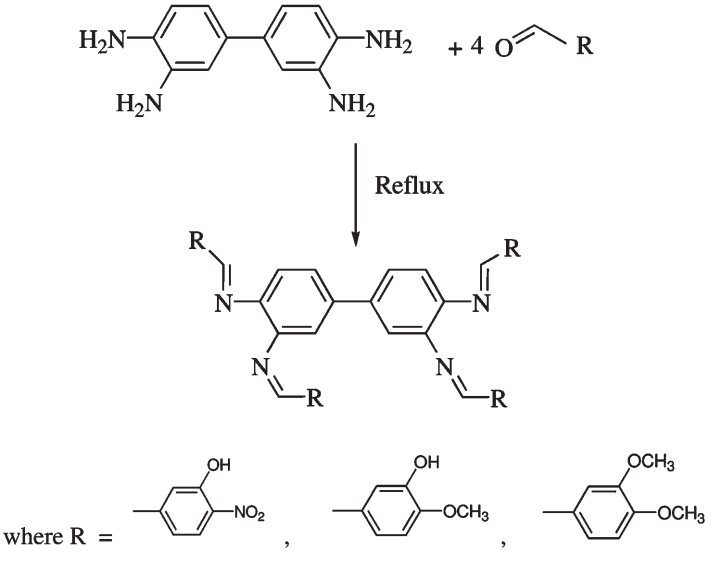

Scheme 1. Outline of the synthesis of ligands.

Cu 11.1, C 52.9, H 4.3, N 5.1. λ_M 10^{-3} ($ohm^{-1}\,cm^2\,mol^{-1}$) 7.8; μ_{eff} (B.M.), 2.85. λ_{max} in DMF, 257, 383, 525, and 914 nm, IC_{50}, 36 μmol dm^{-1}.

Similarly, $[Cu_2(THMBD)Cl_4]$ and $[Cu_2(THNBD)Cl_4]$ were synthesized according to the above-described procedure. $[Cu_2(THMBD)Cl_4]$: Yield: 54%. IR (KBr): 3250–3500 (–OH), 2865 ((methyl)–CH), 1608 (–CH=N) cm^{-1}. *m/z*: 1020, Anal. Calcd for $[Cu_2C_{44}H_{38}N_4O_8Cl_4]$ (%): Cu 12.4, C 51.8, H 3.7, N 5.4; Found (%): Cu 11.9, C 51.2, H 3.7, N 5.4. λ_M 10^{-3} ($ohm^{-1}\,cm^2\,mol^{-1}$), 12.4; μ_{eff} (B.M.), 2.74. λ_{max} in DMF, 262, 392, 544, and 915 nm IC_{50}, 15 μmol dm^{-1}. $[Cu_2(THNBD)Cl_4]$: Yield: 47%. IR (KBr): 3225–3500 (–OH), 1338 (aromatic-NO_2), 1604 (–CH=N) cm^{-1}. *m/z*: 1079, Anal. Calcd for $[Cu_2C_{40}H_{26}N_8O_{12}Cl_4]$ (%): Cu 11.7, C 44.5, H 2.4, N 10.3; Found (%): Cu 11.2, C 44.1, H 2.4, N 10.1. *m/z*: 1010; λ_M 10^{-3} ($ohm^{-1}\,cm^2\,mol^{-1}$), 9.8; μ_{eff} (B.M.), 2.77. λ_{max} in DMF, 252, 394, 547, and 911 nm, IC_{50}, 12 μmol dm^{-1}.

2.5. *Synthesis of [Zn_2(TDBD)Cl_4]*

A solution of TDBD (0.005 mol, 4.03 g) in DMF was added to an ethanolic solution of $ZnCl_2$ (0.01 mol, 1.36 g), the mixture was refluxed for 2 h, concentrated to one-third volume, and kept at 0°C for 10 h. The solid product formed was filtered, washed several times with small amounts of ethanol and diethyl ether, and dried *in vacuo*. Yield: 42%. IR (KBr): 2842 ((methyl)–CH), 1604 (–CH=N) cm^{-1}. ^{1}H-NMR (DMSO-d_6): (phenyl multiplet) 6.4–7.2 δ(m), δ(OCH_3) 3.9(s), (–CH=N) 7.9(s): *m/z*: 1079. Anal. Calcd for $[Zn_2C_{48}H_{46}N_4O_8Cl_4]$ (%): Zn 11.1, C 53.4, H 4.3, N 5.1; Found (%): Zn 10.9, C 52.8, H 4.3, N 5.1. λ_M 10^{-3} ($ohm^{-1}\,cm^2\,mol^{-1}$), 4.8; λ_{max} in DMF, 265 and 372 nm, IC_{50}, 56 μmol dm^{-1}.

Similarly, $[Zn_2(THMBD)Cl_4]$ and $[Zn_2(THNBD)Cl_4]$ were synthesized according to the above-described procedure. $[Zn(THMBD)Cl_4]$: Yield: 28%. IR (KBr): 3250–3500 (–OH), 2838 ((methyl)–CH), 1610 (–CH=N) cm^{-1}. ^{1}H-NMR (DMSO-d_6): (phenyl multiplet) 6.5–7.2 δ(m), (OCH_3) 3.8 δ(s), (–CH=N) 7.7 δ(s) and (–OH) 11.9 δ(s): *m/z*: 1023. Anal. Calcd for $[Zn_2C_{44}H_{38}N_4O_8Cl_4]$ (%): Zn 12.7, C 51.6, H 3.7, N 5.4; Found (%): Zn 12.1, C 50.7, H 3.7, N 5.4. λ_M 10^{-3} ($ohm^{-1}\,cm^2\,mol^{-1}$), 11.9; λ_{max} in DMF, 279 and 368 nm, IC_{50}, 65 μmol dm^{-1}: $[Zn_2(THNBD)Cl_4]$: Yield: 32%. IR (KBr): 3225–3500 (–OH), 1338 (aromatic-NO_2), 1601 (–CH=N) cm^{-1}. ^{1}H-NMR (DMSO-d_6): (phenyl multiplet) 6.5–7.2 δ(m), (–CH=N) 8.3(s) and (–OH) 12.5(s) *m/z*: 1083. Anal. Calcd for $[Zn_2C_{40}H_{26}N_8O_{12}Cl_4]$ (%): Zn 12.0, C 44.3, H 2.4, N 10.3; Found (%): Cu 11.8, C 44.1, H 2.4, N 10.3. λ_M 10^{-3} ($ohm^{-1}\,cm^2\,mol^{-1}$), 15.4; λ_{max} in DMF, 248, 385 nm, IC_{50}, 49 μmol dm^{-1}.

2.6. *DNA cleavage study*

The extent of the cleavage of supercoiled (SC) pUC19 DNA (33.3 μmol, 0.2 μg) to its nicked circular (NC) form was determined by an agarose gel electrophoresis in 5 mmol Tris-HCl buffer (pH 7.2) containing 50 mmol NaCl. For the photo-induced DNA cleavage, the reactions were carried out irradiated at 360 nm. After exposure to light, each sample was incubated for 1 h at 37°C and analyzed for photocleaved products using gel electrophoresis as discussed below. Inhibition reactions for the "chemical nuclease" reactions were carried out in the dark by adding reagents (distamycin, 50 μmol; DMSO, 4 μL) prior to the addition of the complexes and the reducing agent

3-mercaptopropionic acid (MPA). The inhibition reactions for the photo-induced DNA were carried out at 360 nm using NaN_3 (100 μmol) and DMSO (4 μL) prior to the addition of the complexes. For the D_2O experiment, this solvent was used for the dilution of the sample to 18 μL; samples after incubation for 1 h at 37°C in a dark chamber were added to the loading buffer containing 25% bromophenol blue, 0.25% xylene cyanol, 30% glycerol (3 μL), and the solution was finally loaded on 0.8% agarose gel containing 1 μg mL^{-1} ethidium bromide. Electrophoresis was carried out in a dark chamber for 3 h at 50 V in Tris-HCl–EDTA buffer. Bands were visualized by UV light and photographed.

2.7. *Antimicrobial activity*

The *in vitro* biological screening of the investigated compounds were tested against the bacteria *Salmonella typhi*, *Staphylococcus aureus*, *Escherichia coli*, and *Bacillus subtilis* by the well-diffusion method [18] using agar nutrient as the medium and streptomycin as the standard. Antifungal activities were evaluated by the well-diffusion method against the fungi *Aspergillus niger*, *Aspergillus flavus*, *Candida Albicans*, and *Rhizoctonia bataticola* cultured on potato dextrose agar as medium and nystatin as the standard. The stock solution (10^{-2} mol) was prepared by dissolving the compounds in DMSO and the solutions were serially diluted in order to find the minimum inhibitory concentrations (MICs). In a typical procedure [19], a well was made on the agar medium inoculated with microorganisms. The well was filled with the test solution using a micropipette and the plate was incubated, 24 h for bacteria and 72 h for fungi at 35°C. During this period, the test solution diffused and the growth of the inoculated microorganisms was affected. The inhibition zone was developed, at which the concentration was noted.

2.8. *SOD activity*

The SOD activity of the complexes was assayed using nitroblue tetrazolium chloride (NBT) as reported previously [20]. The concentration of complex required to yield 50% inhibition of the reduction of NBT (named IC_{50}) was determined.

3. Results and discussion

The ligands and their complexes are stable in air and soluble only in DMF and DMSO. Elemental analysis data of all ligands and complexes are in agreement with the presented formulae. The physico-chemical and spectroscopic studies presented here indicate the formation of bimetallic complexes of stoichiometry $[M_2LCl_4]$ where L is a ligand possessing four azomethine group (CH=N–) endocyclic substituents, a mimic to cisplatin [21].

3.1. *Mass spectra*

The FAB-mass spectra of synthesized ligands and their complexes were recorded and the obtained molecular ion peaks confirm the proposed formulae. The mass spectrum of ligand shows a peak at m/z 807 (12.5%) corresponding to $[C_{48}H_{46}N_4O_8]^+$ ion. Also, the spectrum exhibited the fragments at m/z 404, 260, 75, and 31 corresponding to $(C_{24}H_{23}N_2O_4)$, $[C_9H_{10}O_2]^+$, $[C_6H_3]^+$, and $[OCH_3]^+$, respectively. The mass spectrum of $[C_{48}H_{46}N_4O_8Cu_2Cl_4]$ shows peaks at 1076, 934, 807, and 404 with 9.2%, 3.5%, 7.4%, and 15.7% abundances, respectively. The one at 1076 may represent the molecular ion peak of the complex and the other peaks are isotopic species. The strongest peak (base peak) at m/z 404 represents the stable species $(C_{24}H_{23}N_2O_4)$. Also, the spectrum exhibited fragments at m/z 260, 75, and 31 corresponding to $[C_9H_{10}O_2]^+$, $[C_6H_3]^+$, and $[OCH_3]^+$, respectively. Thus, the mass spectral data confirm the stoichiometry of the complexes as being of $[M_2LCl_4]$, further supported by the FAB-mass study of other complexes. This stoichiometry is further supported by the elemental analyses, which are in close agreement with the values calculated from molecular formulae assigned to the complexes.

3.2. *Infrared spectra*

IR spectra provide valuable information regarding the nature of the functional group attached to the metal. In the IR spectra of the Schiff bases, a sharp band at 1620–1640 cm^{-1} is assigned to ν(C=N) of azomethine. This band shifts to lower wave numbers ($\sim$25 cm^{-1}) in all the complexes, suggesting the coordination of the azomethine nitrogen to the metal, further substantiated by the presence of a new band at 410–480 cm^{-1}, assigned to ν(M–N) [22]. THMBD and THNBD show a broad band for –OH at *ca* 3250–3500 cm^{-1}. The appearance of this peak in copper and zinc complexes indicates that chelation does not take place *via* –OH. Weak bands were observed in the free ligand spectrum at 2350 cm^{-1}, attributed to C–H vibrations. Further, an intense band at 750 cm^{-1} is typical of aromatic ring vibrations. As expected, these bands are not affected by chelation.

3.3. *Electronic absorption spectra*

The electronic absorption spectra of the complexes were recorded in DMF. The Cu(II) complexes show two bands in the visible region, 10,940–10,976 and 18,281–19,047 cm^{-1}, which are assigned to $^2B_{1g} \rightarrow {}^2A_{1g}$ and $B_{1g} \rightarrow {}^2E_g$ transitions, respectively. The electronic spectral data suggest a square-planar geometry around Cu(II) ion. The electronic absorption spectra of the Zn(II) complexes show bands (25,974–27,173 and 35,842–40,322 cm^{-1}) assigned to intraligand charge transfer transitions [23].

3.4. *Magnetic susceptibility*

The majority of Cu(II) complexes [24] are square-planar or distorted-octahedral. In the case of square-planar, tetrahedral, or distorted-octahedral Cu(II) complexes, the room temperature magnetic moment values are usually observed as 1.8–2.2 B.M. [25] and are

not affected appreciably by the temperature and magnetic field. In practice, compounds whose geometry approaches octahedral usually exhibit magnetic moments at the lower end of the range, while those with square-planer or tetrahedral geometry are at the higher end. For square-planar dimeric or polynuclear species, the complexes display subnormal magnetic moments [25]. The observed room temperature magnetic moment of Cu(II) complexes in the present case is 2.74–2.85 B.M. The spacer [26] nature of the ligand, being two azomethine nitrogens of benzidine moiety far apart, and the analytical data coupled with the magnetic moment suggest that the complex is binuclear [27] with square-planar geometry at each metal center.

3.5. *Nuclear magnetic resonance spectra*

^{1}H-NMR spectra of ligands and their zinc complexes were recorded in DMSO-d_6. TDBD gives the following signals: phenyl as multiplet at 6.4–7.2, –OCH_3 at 3.9, and –CH=N– at 8.1 δ. THMBD and THNBD give phenyl as multiplet at 6.5–7.2, –OCH_3 at 3.8, and –CH=N– at 7.9 and 8.5, and 12.5 and 11.9 δ, which are attributable to the phenolic –OH present in 3-hydroxy-4-nitro benzaldehyde and 4-hydroxy-3-methoxy benzaldehyde. The presence of the phenolic –OH proton for the zinc complex confirms the –OH free from complexation. The azomethine (–N=CH–) proton signal in the zinc complex is shifted downfield compared to the free ligand, suggesting the deshielding of the azomethine due to the coordination with metal. There was no appreciable change in the other signals of the complex.

The decoupled ^{13}C NMR spectra of TDBD and its zinc complex (in DMSO-d_6) confirm the presence of azomethine (–C=N–) and –OCH_3. In zinc complex, the imine carbon was deshielded compared to the free ligand, suggesting the coordination of azomethine nitrogen. Comparison of all other macrocyclic carbon peaks of the ligand with those of the zinc complex [Zn_2LCl_4] shows some upfield and downfield shifts, which are not significant. The data for the free ligand and its zinc complex given in "Supplementary material" are in good agreement with the assigned structure of the ligand and its complexes. Based on the above spectral and analytical data, the structure of the Schiff-base complexes is represented in figure 1.

3.6. *DNA binding studies*

3.6.1. Absorption titration. Electronic absorption spectroscopy is a powerful technique for probing metal ion DNA interactions. Binding of the macromolecule leads to

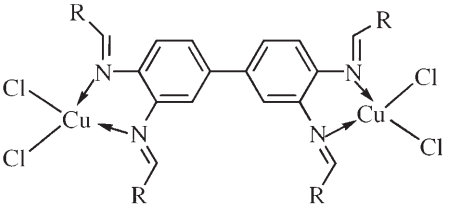

Figure 1. The proposed structure of the Schiff-base complexes.

changes in the electronic spectrum of the metal complex. Base binding is expected to perturb the ligand field transition of the metal complex. Intercalative mode of binding usually results in hypochromism and bathochromism due to the strong stacking interaction between an aromatic chromophore and the base pairs of DNA. The extent of hypochromism parallels the intercalative binding strength. On the other hand, metal complexes which bind non-intercalatively or electrostatically with DNA may result in hyperchromism or hypochromism.

Electronic absorption spectra of $[Cu_2(TDBD)Cl_4]$ in the presence of increasing amounts of CT-DNA in 5 mmol Tris–HCl, 50 mmol NaCl, pH 7.2 buffer is shown in figure 2. In the UV region, the intense absorption bands with a maxima of 383.5 nm for $[Cu_2(TDBD)Cl_4]$, 392 nm for $[Cu_2(THMBD)Cl_4]$, 394 nm for $[Cu_2(THNBD)Cl_4]$, 372 nm for $[Zn_2(TDBD)Cl_4]$, 368 nm for $[Zn_2(THMBD)Cl_4]$, and 385 nm for $[Zn_2(THNBD)Cl_4]$ complexes were attributed to intraligand π–π^* transition. Increasing the concentration of CT-DNA resulted in hypochromism and blueshift in the UV spectrum of the copper complex, suggesting that copper complex binds to DNA by an intercalative mode. After intercalating the base pairs of DNA, the π^* orbit of the intercalated ligand could couple with the π orbital of base pairs, decreasing the π–π^* transition energy and resulting in blueshift. The coupling of π orbit was partially filled by electrons, thus decreasing the transition probabilities and concomitantly resulting in hypochromism. A similar type of binding mode was observed for other complexes with CT-DNA (table 1).

In order to compare the binding strength of the complexes with CT-DNA, the intrinsic binding constants (K_b) are obtained by monitoring the changes in the absorbance for the complexes with increasing the concentration of DNA. The K_b values are shown in table 1.

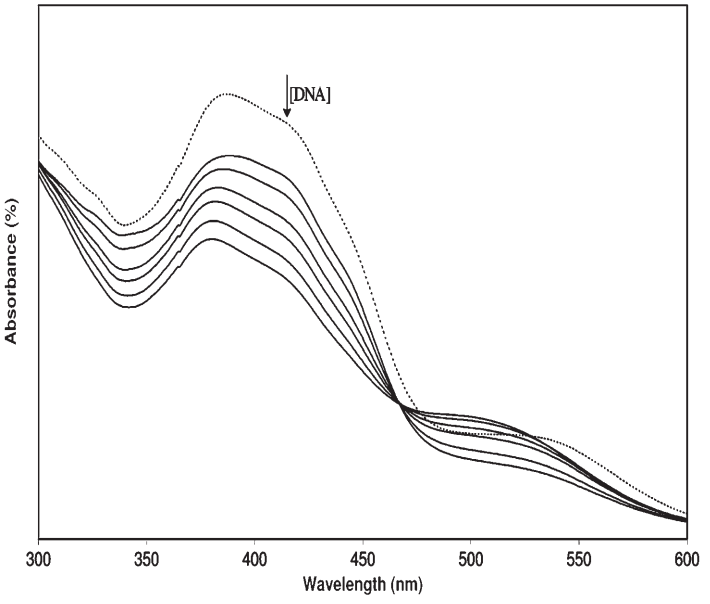

Figure 2. Electronic absorption spectrum of $[Cu_2TDBDCl_4]$ in the absence (dash line) and presence (dark line) of increasing amounts of DNA.

3.6.2. Electrochemical studies. Electrochemical methods to study the metallointercalation and coordination of transitional metal complexes to DNA provide a useful complement to UV-Vis spectroscopy [28]. Typical cyclic voltammograms of $[Cu_2(TDBD)Cl_4]$ in the absence and in presence of varying amounts of [DNA] are shown in figure 3.

In the absence of DNA, the first redox couple cathodic peak appears at −0.412 V for Cu(III) → Cu(II) ($Ep_a = -0.393$ V, $Ep_c = -0.412$ V, $\Delta Ep = 0.019$ V, and $E_{1/2} = -0.403$ V) and second redox couple cathodic peak appears at −0.997 V for Cu(II) → Cu(I) ($Ep_a = -0.982$ V, $Ep_c = -0.97$ V, $\Delta Ep = 0.012$ V, and $E_{1/2} = -0.976$ V). These two redox couples ratio of ip_c/ip_a is approximately unity. This indicates that the reaction of the complex on the glassy carbon electrode surface is quasi-reversible. Incremental addition of DNA to the complex for the second redox couple causes a negative shift in $E_{1/2}$ of 36 mV and a decrease in ΔEp of 23 mV. The ip_c/ip_a values also decreases in the presence of DNA in first couple (Cu(III) → Cu(II)), but in second couple (Cu(II) → Cu(I)) it increases. Peak potentials, Ep_c and Ep_a, as well as $E_{1/2}$ shift to more negative potential, indicating a binding interaction between the complex and DNA that makes the complexes less readily reducible. Changes of the voltammetric currents in the presence of CT-DNA can be attributed to the diffusion of the metal complex bound to the large, slowly diffusing DNA molecule. The changes of the peak currents observed for the complexes upon the addition of CT-DNA may indicate that [THNBD] and [THMBD] complexes possess higher DNA-binding affinity than the other complexes. The results parallel the above spectroscopic and viscosity data of the complexes in the presence of DNA.

Zn(II) complexes show only the oxidation peak from −1.2 to −1.12 V (Ep) and no reduction peak in the absence of DNA. Incremental addition of DNA on Zn(II) complexes shows a decrease in the current intensity and negative shift of the oxidation peak potential. The resulting changes in the current and potential demonstrate the interaction between Zn(II) and DNA. The electrochemical parameters of the Cu(II) and Zn(II) complexes are shown in tables 2 and 3, respectively. According to these data, all the Cu(II) and Zn(II) complexes interact with DNA through intercalation.

Differential pulse voltammograms of $[Cu_2(TDBD)Cl_4]$ in the absence and presence of varying amount of [DNA] are given in figure 4. Increase in the concentration of DNA causes a negative potential shift along with a significant increase of current intensity. The shift in potential is related to the ratio of binding constant

$$E^{o}_{b'} - E^{o}_{f'} = 0.0591 \log(K_+/K_{2+}), \quad (2)$$

Table 1. Absorption spectral properties of complexes with DNA.

Complexes	λ_{max} Free	λ_{max} Bound	$\Delta\lambda$ (nm)	Hypochromicity H (%)	$K_b \times 10^5$ (M^{-1})
$[Cu_2(TDBD)Cl_4]$	383.5	376.0	7.5	5.8	3.2
$[Cu_2(THMBD)Cl_4]$	392	384.0	8.0	7.1	4.7
$[Cu_2(THNBD)Cl_4]$	394	381.5	12.5	9.3	5.8
$[Zn_2(TDBD)Cl_4]$	372	367.5	5.5	5.2	2.6
$[Zn_2(THMBD)Cl_4]$	368	361.0	7.0	6.4	3.9
$[Zn_2(THNBD)Cl_4]$	385	373.0	10.0	8.1	4.3

where $E^{o}_{b'}$ and $E^{o}_{f'}$ are formal potentials of the Cu(II)/Cu(I) complex couple in the bound and free form, respectively. The ratio of the binding constants (K_{+}/K_{2+}) for the DNA binding of Cu(II)/Cu(I) complexes were calculated and found to be less than unity (table 2). This indicates that the binding of Cu(I) complex to DNA is small compared to that of the Cu(II) complex. The above electrochemical results indicate the preferential stabilization of Cu(II) form over Cu(I) form on binding to DNA. The possible mechanism is shown below.

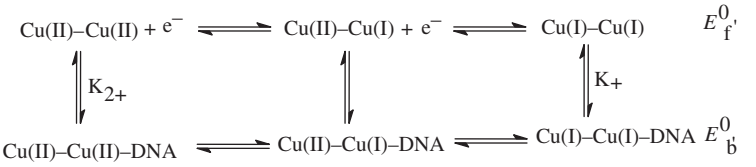

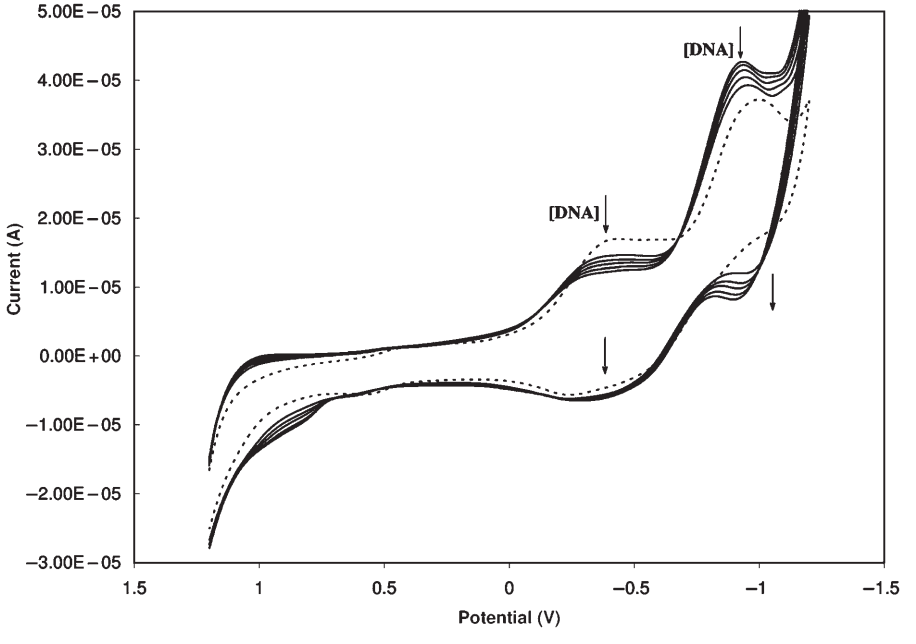

Figure 3. Cyclic voltammogram of $[Cu_2TDBDCl_4]$ both in the absence (dash line) and presence (dark line) of different concentrations of DNA.

Table 2. Electrochemical parameters for the interaction of DNA with Cu(II) complexes.

		$E_{1/2}$ (V)		ΔEp (V)			
Complexes	Redox couple	Free	Bound	Free	Bound	K[red]/K[oxd]	ip_c/ip_a
$[Cu_2(TDBD)Cl_4]$	Cu(III)/Cu(II)	−0.403	−0.375	0.019	0.030	4.4	0.90
	Cu(II)/Cu(I)	−0.976	−0.940	0.012	0.035	0.6	0.75
$[Cu_2(THMBD)Cl_4]$	Cu(III)/Cu(II)	−0.394	−0.313	0.025	0.044	1.9	0.87
	Cu(II)/Cu(I)	−0.970	−0.932	0.012	0.040	0.7	0.85
$[Cu_2(THNBD)Cl_4]$	Cu(III)/Cu(II)	−0.399	−0.308	0.024	0.039	2.3	0.82
	Cu(II)/Cu(I)	−0.958	−0.907	0.013	0.028	0.8	0.92

Differential pulse voltammograms of the Zn(II) complexes have a negative potential shift along with a significant decrease of current intensity during the addition of increasing amounts of DNA, indicating that zinc ions stabilize the duplex (GC pairs) by intercalation. Hence, for the complexes of Zn(II) with DNA, the electrochemical reduction reaction can be divided into two steps:

$$Zn^{2+} - DNA \rightleftharpoons Zn^{2+} + DNA$$

$$Zn^{2+} + 2e^{-} \rightleftharpoons Zn^{0}$$

The dissociation constant (K_d) of the Zn(II)–DNA complex was obtained using the following equation:

$$i_p^2 = \frac{k_d}{[DNA]}(i_{p^o}^2 - i_p^2) + i_{p^o}^2 - [DNA] \quad (3)$$

Table 3. Electrochemical parameters for the interaction of DNA with Zn(II) complexes.

	*E*p (V)		*i*p (A)		
Complexes	Free	Bound	Free	Bound	$K_d \times 10^{-10}$ (mol L^{-1})
$[Zn_2(TDBD)Cl_4]$	−0.65	−0.58	0.42	0.34	6.7
$[Zn_2(THMBD)Cl_4]$	−0.71	−0.63	0.15	0.09	8.6
$[Zn_2(THNBD)Cl_4]$	−0.87	−0.75	0.54	0.43	0.9

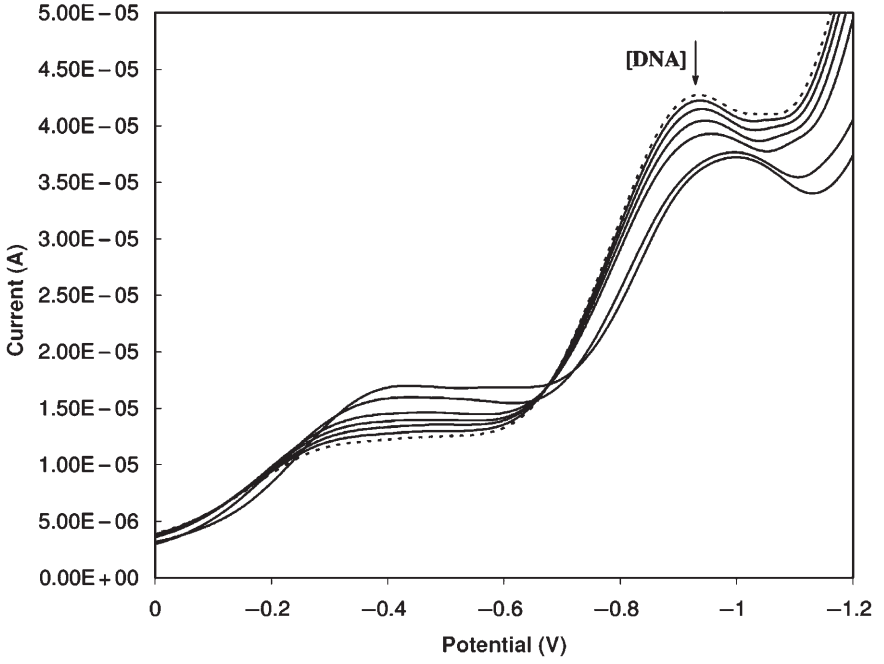

Figure 4. Differential pulse voltammogram of $[Cu_2TDBDCl_4]$ in the absence and presence of different concentrations of DNA.

where K_d is dissociation constant of the complex Zn(II)–DNA and $i_{p^o}^2$ and i_p^2 are the reduction current of Zn(II) in the absence and presence of DNA, respectively. Using equation (3), the dissociation constant was determined. The low dissociation constant values (table 3) of Zn(II) ions were indispensable for the catalytic function and structural stability of zinc enzymes which participate in the replication, degradation, and translation of genetic material of all species. Moreover, Zn(II) ions were probably interacting not only with the active site of the enzyme during these processes, as already well-known in the literature [29], but also with DNA.

3.6.3. Viscosity measurements. To further clarify the interaction between the complexes and DNA, viscosity measurements were carried out. Hydrodynamic measurements that are sensitive to the length change (i.e., viscosity and sedimentation) are regarded as the least ambiguous and the most critical tests of a binding model in solution in the absence of crystallographic structural data. A classical intercalation model demands that the DNA helix lengthen as base pairs are separated to accommodate the binding ligand, leading to an increase in the DNA viscosity. In contrast, a partial and/or non-classical intercalation ligand could bend (or kink) the DNA helix, reduce its effective length, and concomitantly its viscosity. Figure 5 shows the relative viscosity of DNA in the presence of varying amounts of copper and zinc complexes. The relative viscosity steadily increases upon increasing the concentration of zinc or copper complexes. These results suggest that both complexes bind to CT-DNA intercalatively. However, the large increases in the relative viscosity values for THNBD complexes reveal that THNBD complexes are better intercalators than other complexes.

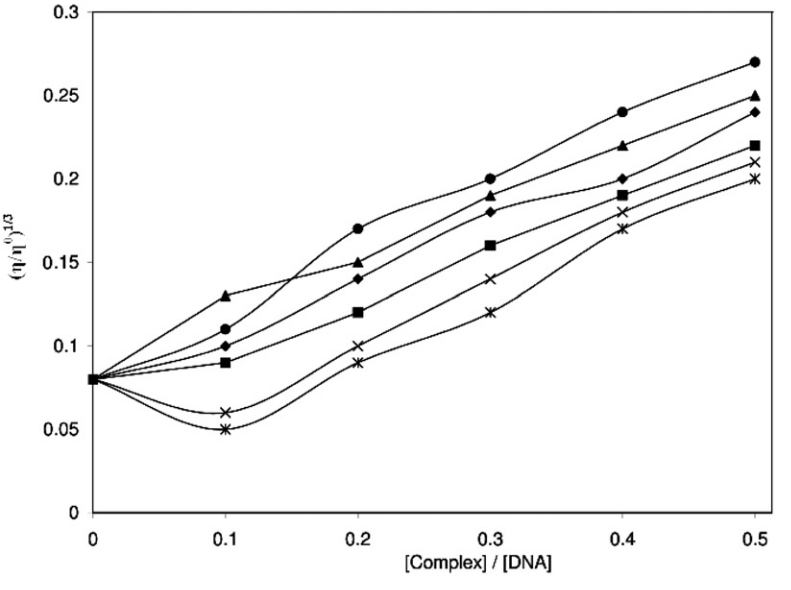

Figure 5. The effect of $[Cu_2THNBDCl_4]$ (▲), $[Zn_2THNBDCl_4]$ (•), $[Cu_2THMBDCl_4]$ (◆), $[Zn_2THMBDCl_4]$ (■), $[Cu_2TDBDCl_4]$ (×), and $[Zn_2TDBDCl_4]$ (*) on the viscosity of DNA; relative specific viscosity *vs.* $R = [complex]/[DNA]$.

3.7. *SOD activity*

The SOD-mimetic activity values (IC_{50}) of synthesized complexes are given in Section 2. On comparing the SOD activities of the present complexes with the reported metal complexes of EDTA and related chelators, our synthesized complexes exhibit significant SOD-mimetic activities (using a modified NBT assay) [30]. In a variety of complexes which act as a SOD enzyme [31], either there is one electron oxidation followed by the reduction of metal ion or the formation of a superoxide complex which then gets reduced to peroxide by another superoxide ion. To explore the mechanism of action, the absorption spectrum of complexes were recorded in the presence and absence of alkaline DMSO (alkaline DMSO acts as a source of O^{2-}). The spectrum got suppressed in alkaline DMSO containing buffer (pH 8.6). However, upon the addition of NBT, which act as O^{2-} scavenger, these peaks were reverted to their original position. Thus, this experiment indicates that O^{2-} is initially attached to the metal complexes, which later get reduced by another O^{2-} ion.

The lower SOD-like activity (IC_{50}) of the copper complexes is due to the weak resistance of these chelates toward O_2^- or the product O_2. The most active metal complexes compare favorably with a number of synthetic SOD mimics developed for therapeutic purposes [32].

3.8. *Chemical nuclease activity*

Chemical nuclease activity is controlled by the relaxation of the SC circular conformation of pUC19 DNA to NC and/or linear conformations. When electrophoresis is applied to a circular plasmid DNA, fastest migration will be observed for the DNA of closed circular conformations (Form I). If one strand is cleaved, the SC will relax to produce a slower-moving nicked conformation (Form II). If both strands are cleaved, a linear conformation (Form III) will be generated that migrates in between [33].

The ligand alone is inactive for DNA cleavage in the presence and absence of any external agents. The oxidative cleavage of pUC19 DNA (Supplementary material) in the presence of an external reducing agent like MPA (5 mmol) (type-I) has been studied by gel electrophoresis using SC pUC19 DNA (0.2 μg, 33.3 μmol) in 5 mmol Tris-HCl/50 mmol NaCl buffer (14 μL, pH 7.2) and the complexes (50 μmol). Control experiments using MPA or the synthesized complexes alone show an apparent cleavage of SC DNA in the dark, suggesting that the complexes bind to DNA. To determine the groove selectivity of the complexes, control experiments are performed using minor groove binder distamycin. The addition of distamycin does not inhibit the cleavage for all the complexes, indicating major groove binding for the synthesized complexes with DNA. Control experiments show that DMSO inhibits DNA cleavage, suggesting the possibility of hydroxyl radical and/or "copper-oxo" intermediate as the reactive species [34]. SOD addition does not have any apparent effect on the cleavage activity, indicating the non-involvement of superoxide radical in the cleavage reaction. The mechanism involved in the DNA cleavage reactions is believed to be similar to that proposed by Sigman *et al.* [35] for the chemical nuclease activity of metal complexes.

3.9. *DNA photo-cleavage study*

Photo-induced DNA cleavage experiments have been carried out in UV light using the Cu(II) and Zn(II) complexes (50 and 100 μmol) and SC pUC19 DNA (0.2 μg, 33.3 μmol) in the absence of any external agent.

The ligand alone is inactive for DNA cleavage. All complexes cleave the pUC19 DNA from its SC to NC form even in the absence of inhibitors on irradiation with UV light at 360 nm. Singlet oxygen quencher, such as sodium azide, inhibits the cleavage. Enhancement of the photo-cleavage of DNA is observed in D_2O in which $^1O_2$ has longer lifetime [36]. Hydroxyl radical scavengers DMSO or KI do not show any significant inhibition in the DNA cleavage activity, indicative of the presence of type-II in which the photo-excited complexes activate molecular oxygen from its stable triplet to the cytotoxic singlet state. Moreover, it suggests the formation of singlet oxygen as the respective species in a type-II process in the metal assisted photo-excitation process involving ligand n–π^* and π–π^* transitions (Supplementary material). The proposed mechanistic pathway for photo-induced cleavage of SC DNA is shown below:

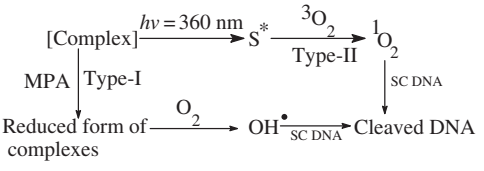

3.10. *Antimicrobial activity*

For *in vitro* antimicrobial activity, the compounds were tested against bacteria and fungi. The MICs are summarized in tables 4 and 5. A comparative study of the ligands and their complexes (MIC values) indicates that complexes exhibit higher antimicrobial activity than the free ligand. From the MIC values, THNBD complexes are more potent than other complexes. Such increased activity of the complexes can be explained on the basis of Overtone's concept [37] and Tweedy's chelation theory [38]. These complexes also disturb the respiration process of the cell and thus block the synthesis of the proteins that restricts further growth of the organism. Furthermore, the mode of action

Table 4. MIC of the compounds against the growth of four fungi (mg mL^{-1}).

Compound	*A. niger*	*A. flavus*	*C. albicans*	*R. bataticola*
TDBD	78	69	63	71
THMBD	65	52	58	74
THNBD	75	68	62	67
$[Cu_2(TDBD)Cl_4]$	42	38	24	36
$[Cu_2(THMBD)Cl_4]$	36	32	28	44
$[Cu_2(THNBD)Cl_4]$	35	27	43	28
$[Zn_2(TDBD)Cl_4]$	38	24	45	37
$[Zn_2(THMBD)Cl_4]$	33	28	47	38
$[Zn_2(THNBD)Cl_4]$	27	30	42	31
Nystatin	10	8	12	14

Table 5. MIC of the compounds against the growth of four bacteria ($mg\,mL^{-1}$).

Compound	*E. coli*	*S. typhi*	*S. aureus*	*B. subtilis*
TDBD	60	71	74	82
THMBD	57	68	71	77
THNBD	47	57	63	73
$[Cu_2(TDBD)Cl_4]$	28	24	32	21
$[Cu_2(THMBD)Cl_4]$	24	32	29	22
$[Cu_2(THNBD)Cl_4]$	14	28	18	22
$[Zn_2(TDBD)Cl_4]$	20	33	22	18
$[Zn_2(THMBD)Cl_4]$	29	32	30	26
$[Zn_2(THNBD)Cl_4]$	18	27	25	23
Streptomycin	14	18	12	10

of the compound may involve the formation of a hydrogen bond through the azomethine group with the active center of cell resulting in interference with the normal cell process and in general metal complexes are more active than the ligands because metal complexes may serve as a vehicle for activation of ligands as the principle cyctotoxic species [39].

4. Conclusions

Three new Schiff bases and their Cu(II) and Zn(II) complexes were synthesized and characterized. They are bimetallic and square-planar geometry around metal(II) ions. The planarity and extended conjugation effect the DNA binding and cleavage activity of the complexes. Mechanistic investigations show a major groove binding for the synthesized macrocyclic complexes with DNA. The synthesized complexes exhibit chemical nuclease activity in the dark in the presence of a reducing agent (MPA) *via* mechanistic pathway involving the formation of hydroxyl radical as the reactive species. Pathways involving singlet oxygen in the DNA photo-cleavage reactions are proposed from the observation of the complete inhibition of the cleavage in the presence of sodium azide and the enhancement of cleavage in D_2O. Hydroxyl radical scavengers like DMSO do not show any significant effect on the DNA cleavage activity, suggesting the formation of singlet oxygen as the reactive species in a type-II process. The synthesized complexes exhibit significant SOD-mimetic activities and have higher antimicrobial activity than the ligands. These binuclear complexes exhibit more SOD, DNA binding (from the DNA binding constants), and cleaving ability (from redox behavior) compared to mononuclear complexes.

Acknowledgments

The authors express their heartfelt thanks to the College Managing Board, VHNSN College, Virudhunagar, for providing research facilities. N. Raman and A. Sakthivel express their gratitude to the UGC, New Delhi, for financial assistance.

References

[1] E. Manoj, M.R. Prathapachandra Kurup, A. Punnoose. *Spectrochim. Acta*, **72A**, 474 (2009).
[2] C. Liu, M. Wang, T. Zhang, H. Sun. *Coord. Chem. Rev.*, **248**, 147 (2004).
[3] F. Mancin, P. Tecilla. *New J. Chem.*, **31**, 800 (2007).
[4] F. Liang, S. Wan, Z. Li, X. Xiong, L. Yang, X. Zhou, C. Wu. *Curr. Med. Chem.*, **13**, 711 (2006).
[5] G. Feng, J.C. Mareque-Rivas, N.H. Williams. *Chem. Commun.*, 1845 (2006).
[6] J. Qian, W. Gu, H. Liu, F. Gao, L. Feng, S. Yan, D. Liao, P. Cheng. *Dalton Trans.*, 1060 (2007).
[7] O. Iranzo, T. Elmer, J.P. Richard, J.R. Morrow. *Inorg. Chem.*, **42**, 7737 (2003).
[8] Q. Li, J. Huang, Q. Wang, N. Jiang, C. Xia, H. Lin, J. Wu, X. Yu. *Bioorg. Med. Chem.*, **14**, 4151 (2006).
[9] S. Wan, F. Liang, X. Xiong, L. Yang, X. Wu, P. Wang, X. Zhou, C. Wu. *Bioorg. Med. Chem. Lett.*, **16**, 2804 (2006).
[10] W.H. Chapman Jr, R. Breslow. *J. Am. Chem. Soc.*, **117**, 5462 (1995).
[11] K.A. Deal, J.N. Burstyn. *Inorg. Chem.*, **35**, 2792 (1996).
[12] N. Raman, R. Jeyamurugan. *J. Coord. Chem.*, **62**, 2375 (2009).
[13] N. Raman, S. Parameswari. *Pol. J. Chem.*, **82**, 1331 (2008).
[14] N. Raman, S. Johnson Raja, A. Sakthivel. *J. Coord. Chem.*, **62**, 691 (2009).
[15] R. Bera, B.K. Sahoo, K.S. Ghosh, S. Dasgupta. *Int. J. Biol. Macromol.*, **42**, 14 (2008).
[16] M.F. Reichmann, S.A. Rice, C.A. Thomas, P. Doty. *J. Am. Chem. Soc.*, **76**, 3047 (1954).
[17] S. Satyanarayana, J.C. Dabrowiak, J.B. Chaires. *Biochemistry*, **31**, 9319 (1992).
[18] O. Irobi, M.M. Young, W.A. Anderson. *Int. J. Pharm.*, **34**, 87 (1996).
[19] M.J. Pelczar, E.C.S. Chan, N.R. Krieg. *Microbiology*, 5th Edn, Blackwell Science, New York (1998).
[20] R.G. Bhirud, T.S. Srivastava. *Inorg. Chim. Acta*, **173**, 121 (1990).
[21] W.S. Browner, A.J. Kahn, E. Ziv, A.P. Reiner, J. Oshima, R.M. Cawthon, W.C. Hsueh, S.R. Cummings. *Am. J. Med.*, **117**, 851 (2004).
[22] D. Kong, J. Wang, L. Zhu, Y. Jin, X. Li, H. Shen, H. Mi. *J. Inorg. Biochem.*, **102**, 824 (2008).
[23] R. Atkins, G. Brewer, E. Kokot, G.M. Mockler, E. Sinn. *J. Inorg. Chem.*, **24**, 127 (1985).
[24] K.S. Patel, J.A.O. Woods. *Synth. React. Inorg. Met.-Org. Chem.*, **20**, 909 (1990).
[25] R.C. Maurya, R. Verma, H. Singh. *Synth. React. Inorg. Met.-Org. Chem.*, **33**, 1063 (2003).
[26] H. Choudhary, R. Ghosh, B.N. Sarkar, S.P. Banerjee, B.K. Gosh. *Indian J. Chem.*, **46A**, 1393 (2007).
[27] K.S. Ganesh, C.N. Krishnan. *Synth. React. Inorg. Met.-Org. Chem.*, **24**, 1789 (1994).
[28] T. Hirohama, Y. Kuranuki, E. Ebina, T. Sugizaki, H. Arii, M. Chikira, P.T. Selvi, M. Palaniandavar. *J. Inorg. Biochem.*, **99**, 1205 (2005).
[29] G.M. Blackburn, M.J. Gait. *Nucleic Acid in Chemistry and Biology*, 2nd Edn, Oxford University Press, New York (1996).
[30] M. Baudry, S. Etienne, A. Bruce, M. Palucki, E. Jacobsen, B. Malfroy. *Biochem. Biophys. Res. Commun.*, **192**, 964 (1993).
[31] A.E.O. Fisher, S.C. Maxwell, D.P. Naughton. *Biochem. Biophys. Res. Commun.*, **316**, 48 (2004).
[32] D.T. Sawyer, J.S. Valentine. *Acc. Chem. Res.*, **14**, 393 (1981).
[33] M.C. Prabahara, H.S. Bhojya Naik. *Biometals*, **21**, 675 (2008).
[34] T.B. Thederahn, M.D. Kuwabara, T.A. Larsen, D.S. Sigman. *J. Am. Chem. Soc.*, **111**, 4941 (1989).
[35] D.S. Sigman, A. Mazumder, D.M. Perrin. *Chem. Rev.*, **93**, 2295 (1993).
[36] A.U. Khan. *J. Phys. Chem.*, **80**, 2219 (1976).
[37] N. Raman, A. Sakthivel, K. Rajasekaran. *J. Coord. Chem.*, **62**, 1661 (2009).
[38] S. Belaid, A. Landreau, S. Djebbar, O. Benali-Baitich, G. Bouet, J.P. Bouchara. *J. Inorg. Biochem.*, **102**, 63 (2008).
[39] D.H. Petering. In *Metal Ions in Biological Systems*, H. Sigel (Ed.), Vol. 2, pp. 167–206, Marcel Dekker, New York (1973).